

International Sherwood Fusion Theory Conference
Madison, WI, April 4-6, 2016

Production and Damping of Runaway Electrons in a Tokamak

Boris Breizman¹⁾ and Pavel Aleynikov²⁾

1) Institute for Fusion Studies, Austin, TX, USA

2) Max-Planck-Institut für Plasmaphysik, Greifswald, Germany

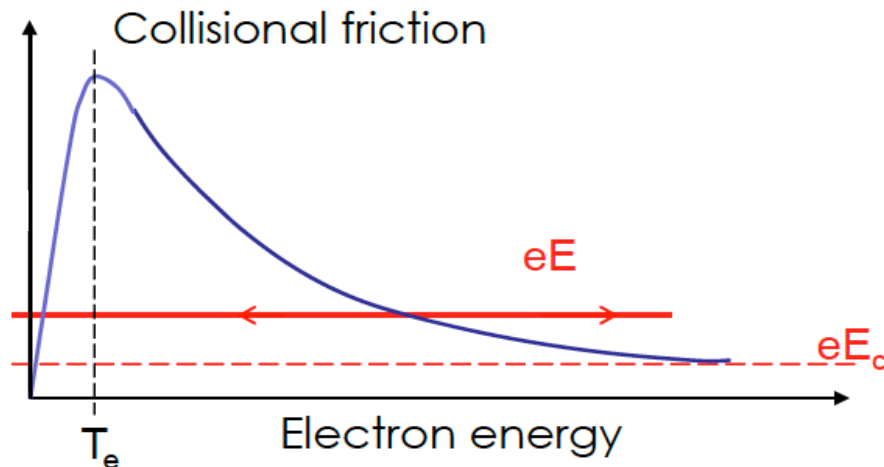
Work supported by the U.S. DOE Contract No.DEFG02-04ER54742
and by ITER contracts ITER-CT-12-4300000273, ITER/CT/15/4300001178

Outline

- ❑ Thermal quench and primary runaway production
- ❑ Runaway avalanche and runaway sustainment
- ❑ Damping of runaway current
- ❑ Micro-instabilities
- ❑ Summary

Runaway production

- ❑ Electrons cool down, plasma becomes more resistive, and loop voltage increases during thermal quench.
- ❑ Strong toroidal electric field produces relativistic runaway electrons.



$$E_c = \frac{4\pi n_e e^3 \Lambda}{mc^2} = 0.075 \times n_{e,20}$$

- ❑ Friction force decreases with energy for nonrelativistic electrons and asymptotes to eE_c at relativistic energies.
- ❑ Critical loop voltage in ITER is about 1V.

Thermal quench model

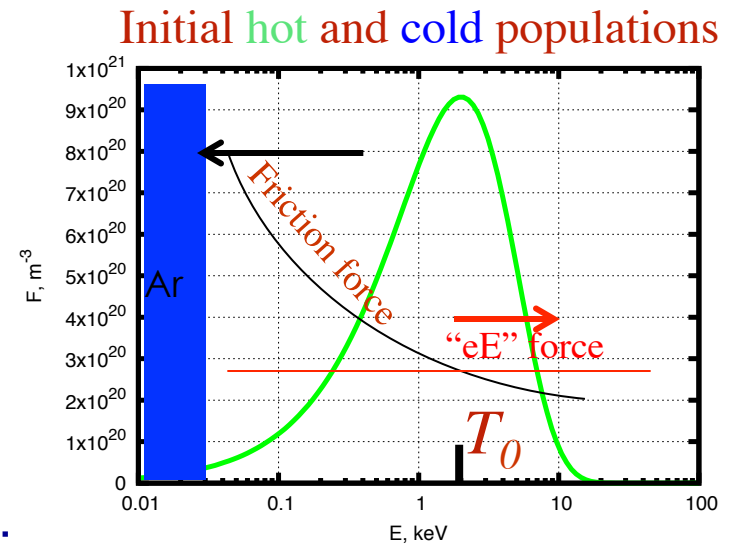
- Maxwellian pre-quench electrons (n_0, T_0) with Spitzer correction (j_0).
- Pellet delivers cold ions ($n_{cold} > n_0$ after ionization).
- Kinetic treatment of the hot electrons: the timescales for collisions are

$$\nu_{cold-cold} \gg \nu_{hot-cold} \gg \nu_{hot-hot}$$

- The current density is constant during TQ; the electric field evolves accordingly:

$$j_0 = \int e v_{\parallel} F(t, E) dp \sin(\theta) d\theta + \sigma_{cold} E(t)$$

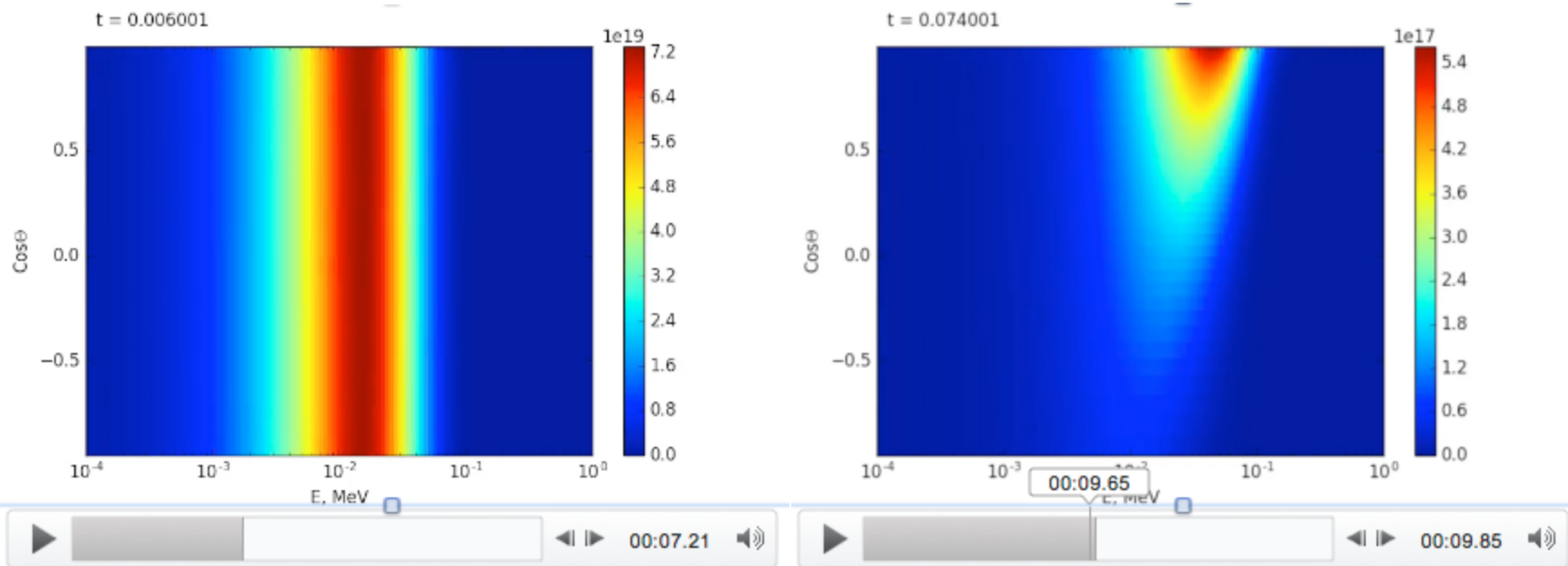
- σ_{cold} is determined by the hot population energy release and line-radiation



2-d evolution of the hot electron distribution

Conservation of the total current precludes complete slowing down of the hot population

The surviving hot electrons form a runaway beam



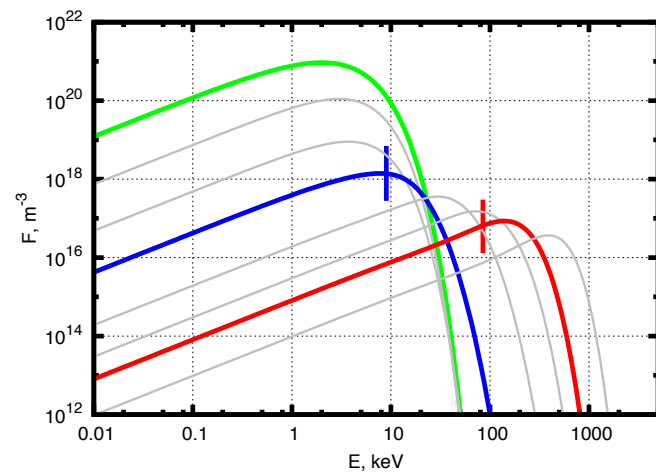
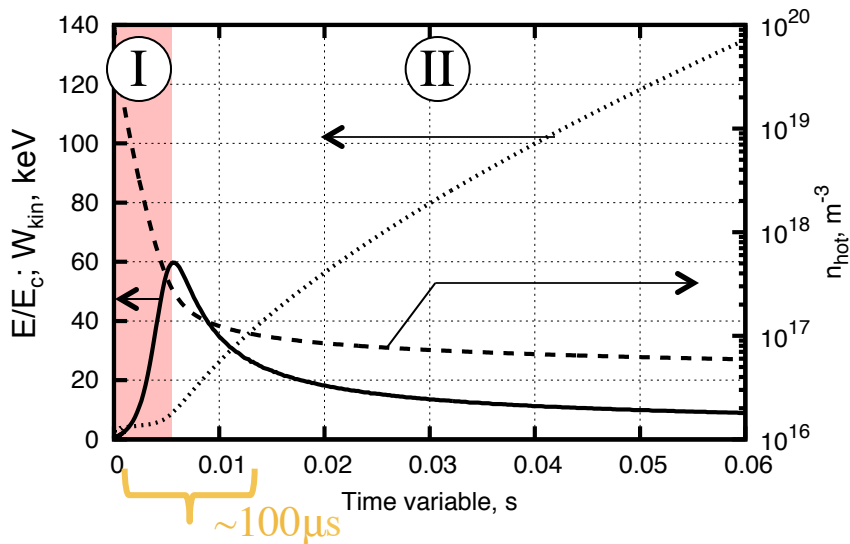
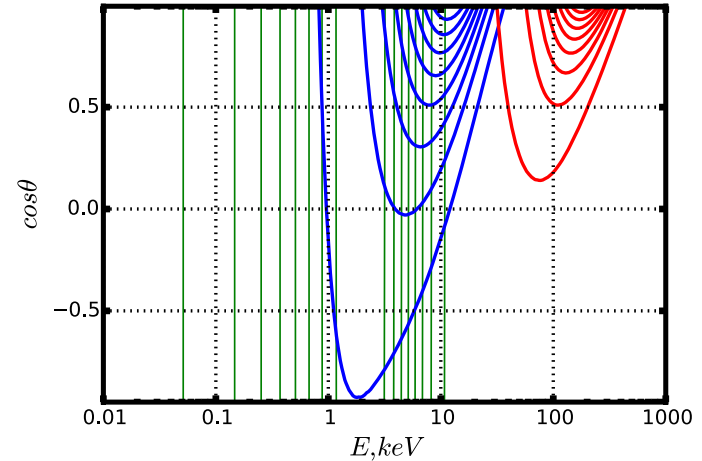
Hot electron survival in the limit of $\sigma_{\text{cold}}=0$

Phase I

- ❑ Electric field rises in step with the loss of the hot population.
- ❑ The remaining hot electrons form a beam; total current is carried by the hot population

Phase II

- ❑ Electric field decays slowly as the surviving electrons accelerate



Seed reduction by bulk conductivity

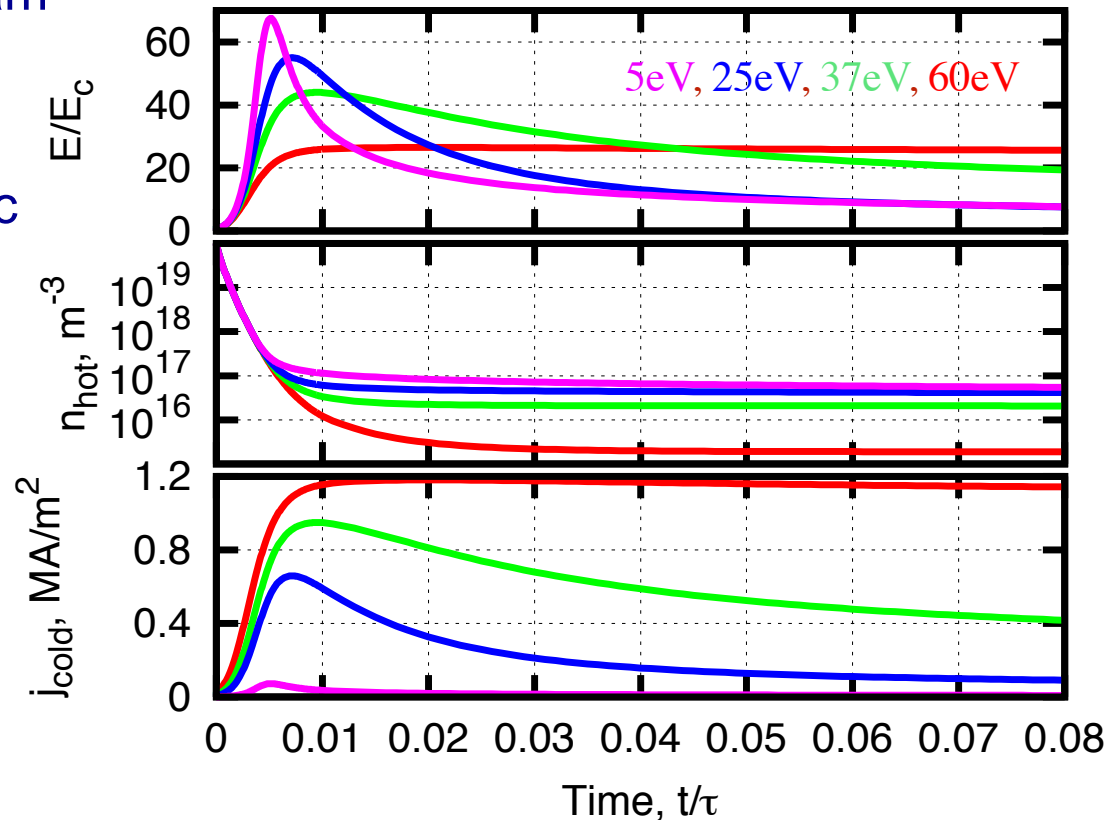
□ If $\sigma_{\text{cold}}=0$, all the post-TQ current is carried by the hot electron beam (no need for the avalanche).

□ Finite σ_{cold} reduces the electric field and makes it more difficult for the hot electrons to survive.

Lower temperature



More “surviving electrons”



Self-consistent thermal quench

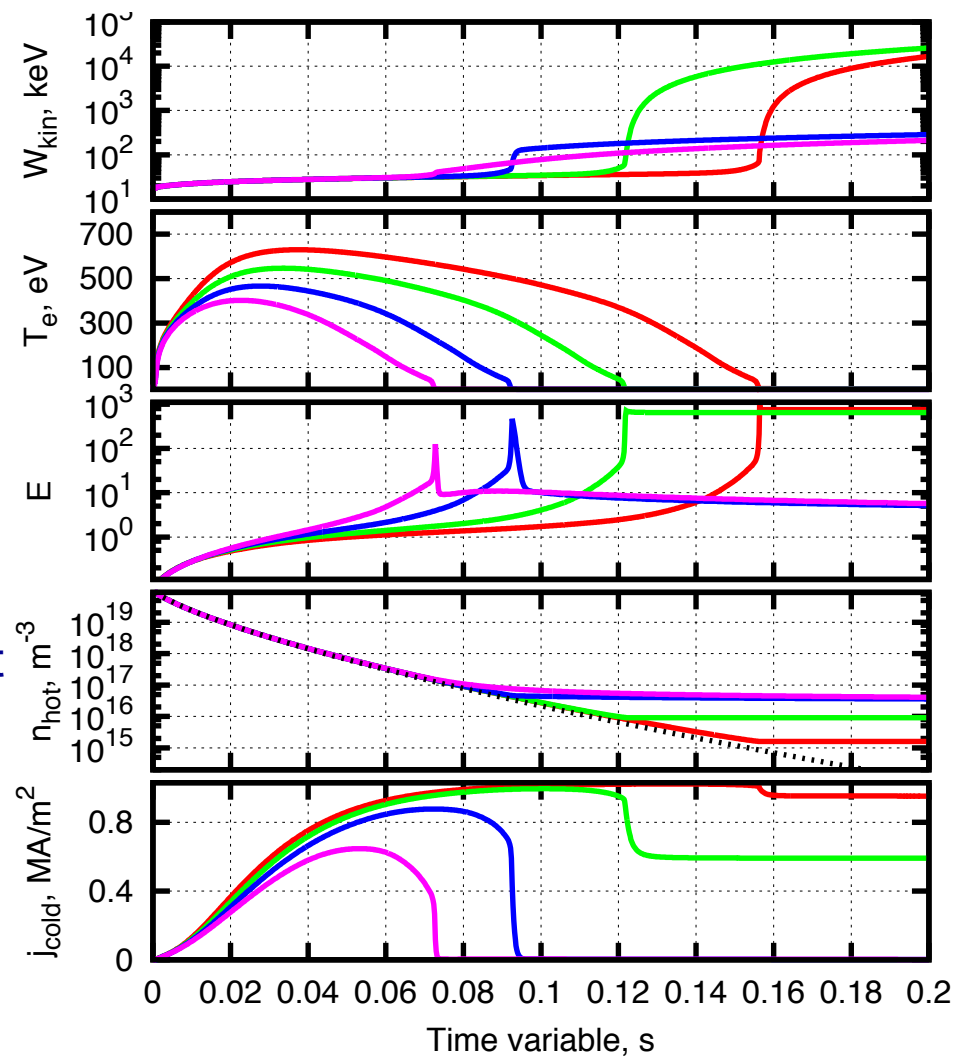
Thermal quench scenario:

- ① Hot electrons heat the “cold” bulk via Coulomb collisions
- ② The bulk overtakes a fraction of the current
- ③ Bulk conductivity drops due to radiative losses. The hot population decreases in the meantime

There are two possible outcomes:

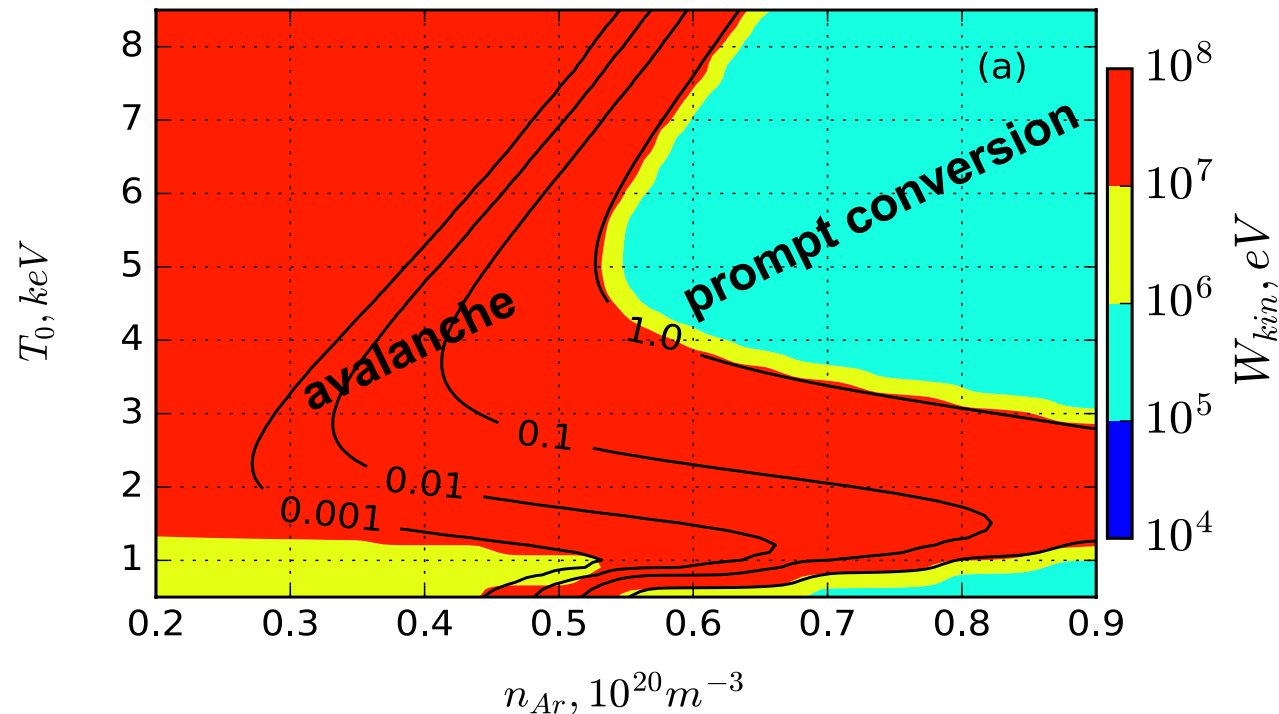
1. **Prompt conversion regime:** purple & blue (low energy REs carry the total current at low electric field).

2. **Seed for avalanche regime:** green & red (Ohmic current -> high electric field -> high energy seed REs for avalanche).



Scan over initial plasma parameters

Contour plot of the surviving hot electron population (normalized to j_{σ}/ec)
The **prompt conversion** area represents 100% of sub-MeV RE current



- ❑ The electric field is supercritical ($E/E_c \sim 4 \div 8$) in the prompt conversion regime (due to relatively slow transformation of the 100keV RE into 1MeV RE current)
- ❑ The seed density has a non-monotonic dependence on pre-quench temperature with a maximum at $T_0 \sim 4$ keV

Summary of runaway seed modeling in DIII-D and ITER

DIII-D:

- ❑ RE seed peaks toward the core, because $T_0 < 5$ keV
- ❑ RE-free disruption for $n_{Ar} < 10^{19} \text{ m}^{-3}$
- ❑ Non-uniformity of the plasma allows the post-quench current to be carried by two distinct runaway populations (sub-MeV and ultra-relativistic).
- ❑ Prompt conversion of the total current into RE current for $n_{Ar} > 0.45 \times 10^{20} \text{ m}^{-3}$
- ❑ High current density ($\sim 3 \text{ MA/m}^2$) facilitates Dreicer generation

ITER-relevant conditions:

- ❑ Non-monotonic RE profile expected, because $T_0 > 5$ keV
- ❑ RE-free disruption for $n_{Ar} < 3 \times 10^{19} \text{ m}^{-3}$
- ❑ Prompt conversion of the total current into RE current for $n_{Ar} > 10^{20} \text{ m}^{-3}$
- ❑ Negligibly weak Dreicer mechanism

Avalanche mechanism

- ❑ Seed runaway electrons produce secondary electrons via large-angle (Möller) collisions with the bulk.
- ❑ The source of secondary electrons is proportional to the density of existing runaways.
- ❑ The runaway population grows exponentially and saturates when it takes large part of the total current

- ❑ Points of interest:
 - ❑ Critical electric field for avalanche onset
 - ❑ Avalanche growth rate
 - ❑ Runaway distribution function

C. Møller, *Ann. Phys. (Leipzig)* **14**, 531 (1932)

Yu. A. Sokolov, *JETP Letters* **29**, 218 (1979)

M. N. Rosenbluth and S. V. Putvinski, *Nucl. Fusion* **37**, 1355 (1997).

Runaway kinetics and separation of time scales

□ Kinetic equation:

$$\frac{\partial F}{\partial t} + eE \left(\frac{1}{p^2} \frac{\partial}{\partial p} p^2 \cos \theta F - \frac{1}{p \sin \theta} \frac{\partial}{\partial \theta} \sin^2 \theta F \right) = \hat{C}F + \hat{R}F + \hat{S}F$$

Small-angle collisions:

$$\hat{C}F = \frac{mc}{\tau} \left(\frac{1}{p^2} \frac{\partial}{\partial p} (p^2 + m^2 c^2) F + \frac{(Z+1) mc \sqrt{p^2 + m^2 c^2}}{2 \sin \theta} \frac{\partial}{\partial \theta} \sin \theta \frac{\partial}{\partial \theta} F \right)$$

Synchrotron radiation reaction:

$$\hat{R}F = \frac{mc}{\tau_{rad}} \left[\frac{1}{m^2 c^2 p^2} \frac{\partial}{\partial p} p^3 \sqrt{m^2 c^2 + p^2} \sin^2 \theta F + \frac{1}{p \sin \theta} \frac{\partial}{\partial \theta} \frac{p \cos \theta \sin^2 \theta}{\sqrt{m^2 c^2 + p^2}} F \right]$$

Knock-on collisions (Möller source): $\hat{S}F$

Time scales:

$$\tau \equiv \frac{m^2 c^3}{4 \pi n_e e^4 \Lambda}$$

$$\tau_{rad} \equiv \frac{3 m^3 c^5}{2 e^4 B^2}$$

□ Möller source ($\hat{S}F$) is weaker than electron drag (by Coulomb logarithm).

□ Two-step description of the runaway avalanche:

- ① Examine sustainment of the runaways in the absence of knock-on collisions
- ② Use the distribution function of the sustained runaways to predict their multiplication or loss due to knock-on collisions.

Source of knock-on electrons

The simplified source [Nucl. Fusion **37**, 1355(1997)] implies **ultra-relativistic primary electrons without angular spread**.

The needs to relax these constraints:

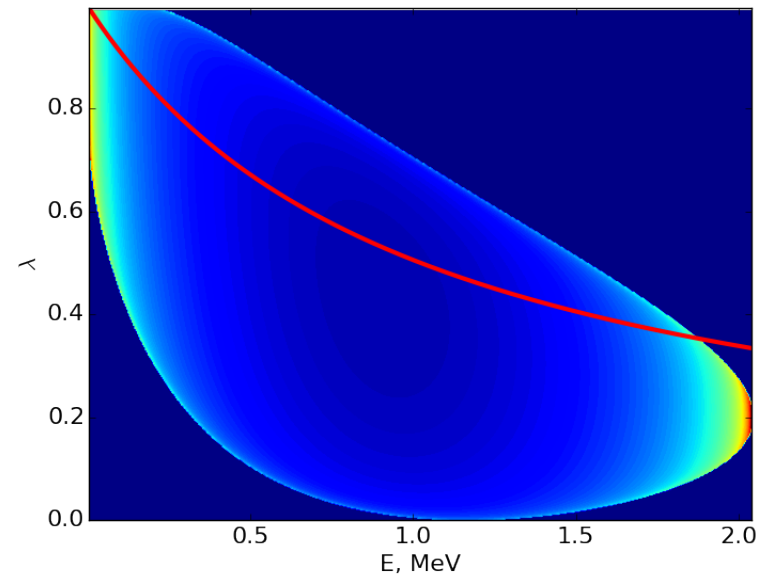
- runaway scattering on high-Z impurities
- energy limitation by synchrotron radiation
- moderate energy of primary electrons at high electric field

$$\text{Exact source : } S = n_{\text{cold}} c \frac{\sqrt{\gamma_0^2 - 1}}{\gamma_0} \langle \delta[\cos\theta - \cos\theta_p] \rangle \frac{d\sigma}{d\Delta}$$

$d\sigma / d\Delta =$ Møller cross-section

The gyro-averaged δ -function is

$$\langle \delta[\cos\theta - \cos\theta_p] \rangle = \frac{1}{\pi} \frac{1}{\sqrt{\left(\frac{p_{\perp} p_{0\perp}}{pp_0}\right)^2 - \left(\frac{p_{\parallel} p_{0\parallel}}{pp_0} - \sqrt{\frac{\gamma-1}{\gamma+1}} \sqrt{\frac{\gamma_0+1}{\gamma_0-1}}\right)^2}}$$



*Red curve - shape of the simplified source.
Color-coded - exact source for primary electrons with $\gamma_0 \approx 5$ and $\lambda_0 = 0.2$.*

Near-threshold ordering

□ The time-scale for pitch-angle equilibration is much shorter than the momentum evolution time-scale **for moderate values of the electric field.**

□ Relatively long synchrotron time-scale ($\bar{\tau}_{rad} \gg 1$).

□ The lowest order kinetic equation is: $\frac{E}{p} F + \frac{(Z+1)\sqrt{p^2+1}}{2} \frac{1}{p^3} \frac{1}{\sin\theta} \frac{\partial F}{\partial\theta} = 0$.

□ Lowest order solution:

$$F = G(t; p) \frac{A}{2 \sinh A} \exp[A \cos\theta]$$

$$A(p) \equiv \frac{2E}{(Z+1)} \frac{p^2}{\sqrt{p^2+1}}$$

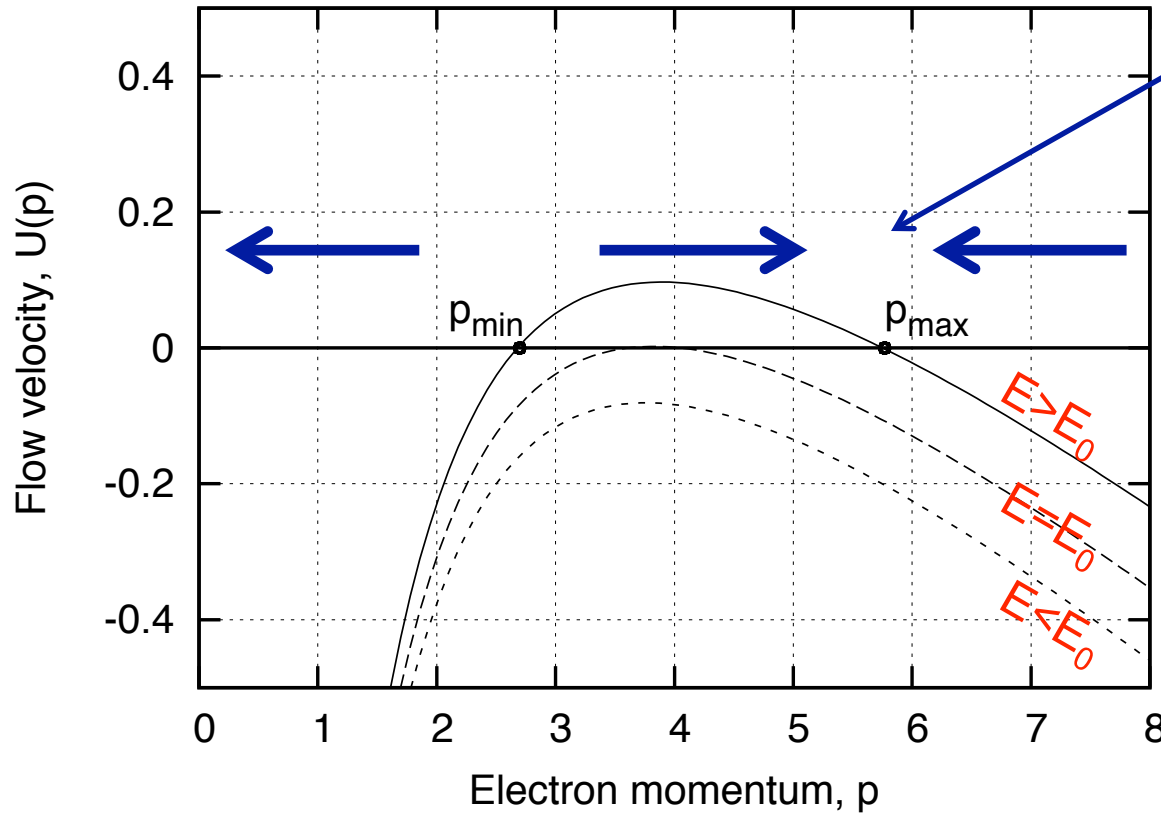
□ Integration of the kinetic equation over all pitch-angles eliminates the lowest order terms and gives a continuity equation in momentum:

$$\frac{\partial G}{\partial t} + \frac{\partial}{\partial p} U(p)G = 0$$

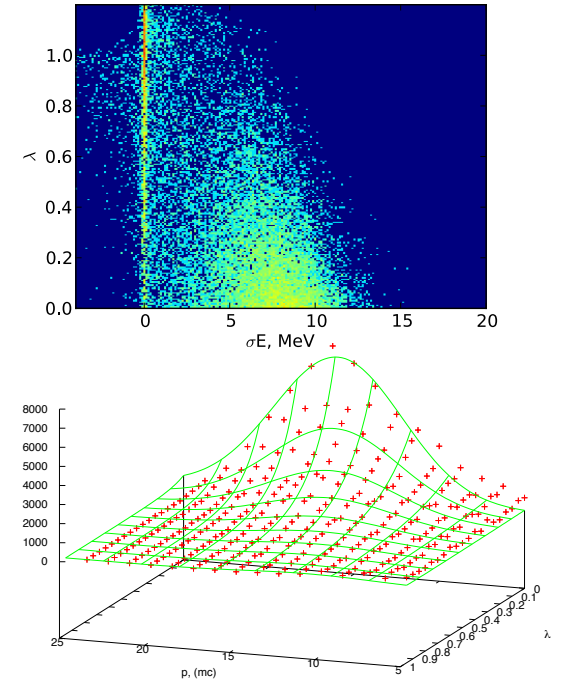
$$U(p) \equiv - \left[\frac{1}{A(p)} - \frac{1}{\tanh(A(p))} \right] E - 1 - \frac{1}{p^2} + \frac{Z+1}{E\bar{\tau}_{rad}} \frac{p^2+1}{p} \left[\frac{1}{A(p)} - \frac{1}{\tanh(A(p))} \right]$$

Momentum space attractor

$$U(p) \equiv - \left[\frac{1}{A(p)} - \frac{1}{\tanh(A(p))} \right] E - 1 - \frac{1}{p^2} + \frac{Z+1}{E\bar{\tau}_{rad}} \frac{p^2+1}{p} \left[\frac{1}{A(p)} - \frac{1}{\tanh(A(p))} \right]$$

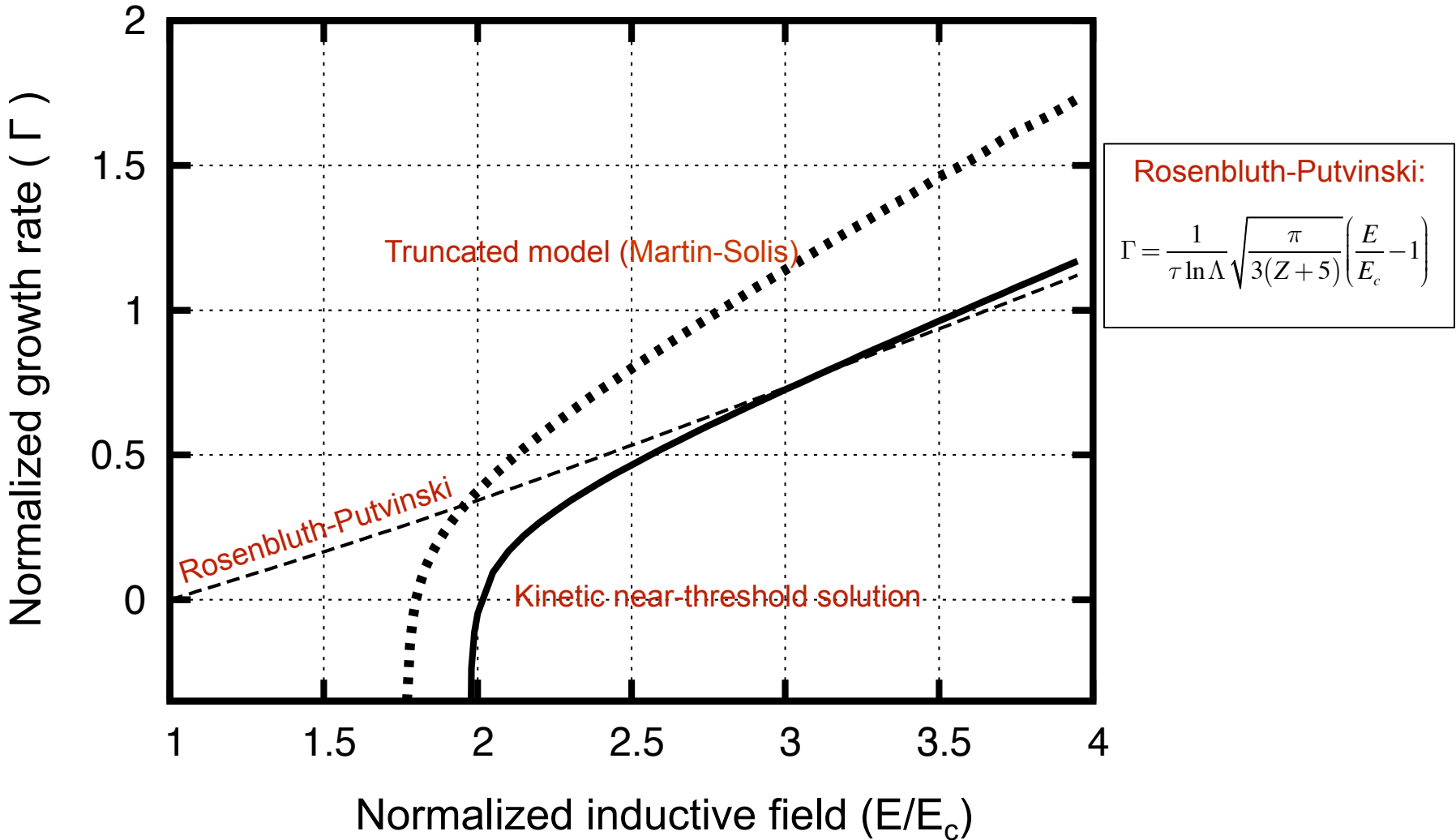


Peaking of the distribution function around p_{\max}



The roots p_{\min} and p_{\max} merge at a certain electric field $E=E_0$. This is the minimal electric field required for runaway sustainment.

Avalanche growth rates comparison



PRL, **114**,155001(2015).

Marginal stability model for runaway current damping

- ❑ Characteristic times of runaway electron stopping and their production via avalanche mechanism are much shorter than the current decay time-scale.
- ❑ The local inductive electric field must be very close to the avalanche threshold to maintain runaway current at any flux surface
- ❑ The threshold electric field is determined by plasma density

$$\frac{1}{r} \frac{\partial}{\partial r} r \frac{\partial E_{\parallel}}{\partial r} = \frac{4\pi}{c^2} \frac{\partial j_{\parallel}}{\partial t} \quad \text{“Ohm’s law”}:$$
$$j_{\parallel} > 0 \Rightarrow E_{\parallel} = E_c(n)$$
$$j_{\parallel} = 0 \Rightarrow E_{\parallel} < E_c(n)$$

Dynamics of the runaway current profile

❑ Critical field: $E_c = \frac{4\pi n_e e^3 \Lambda}{mc^2} \equiv E_0 \left(1 - \frac{r^2}{a^2}\right)$

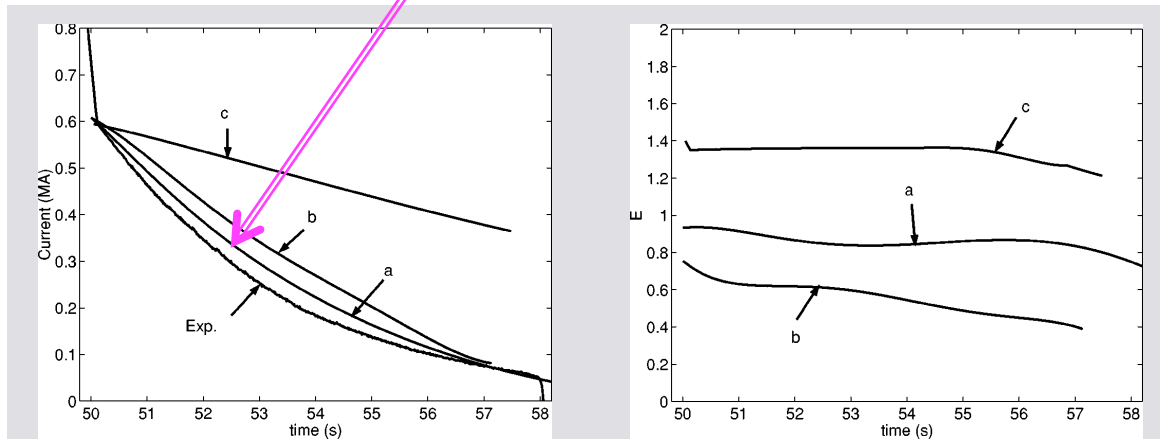
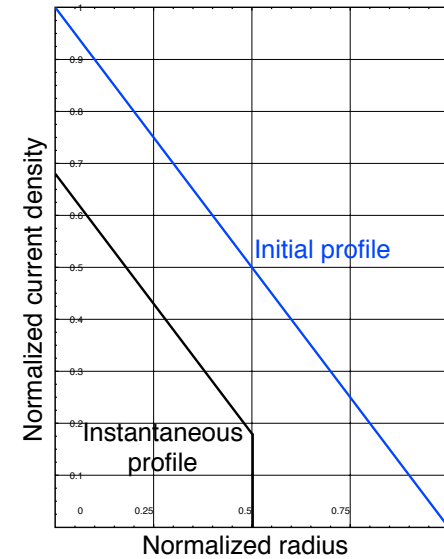
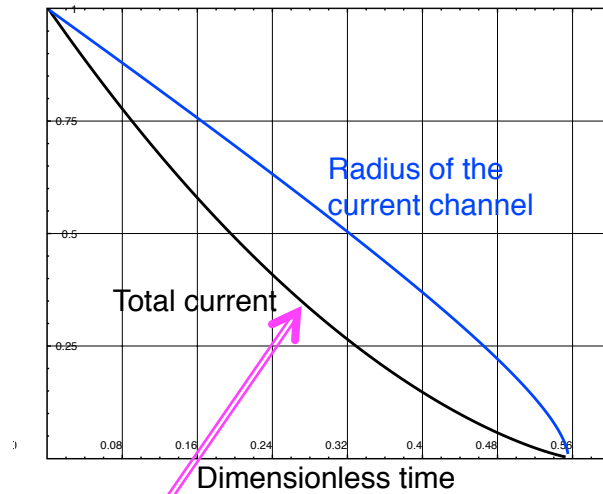
❑ Initial current profile: $j = j_0 \left(1 - \frac{r}{a}\right)$

❑ Time-scale of current decay: $t_{decay} = \frac{\pi j_0 a^2}{c^2 E_0}$

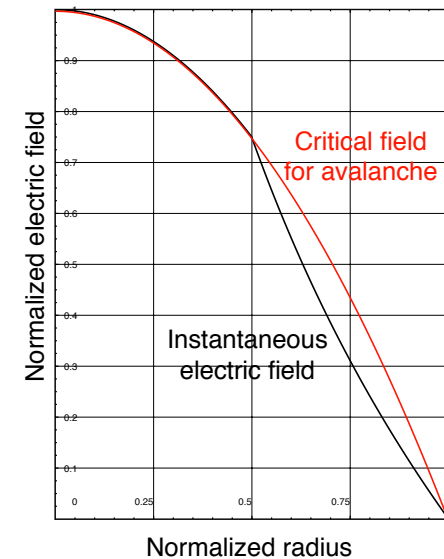
❑ The current density decreases and the current channel narrows over time:

$$\frac{d\rho}{d\tau} = \frac{1 - \rho^2 + 2\rho^2 \ln \rho}{4\rho(1 - \rho - \tau) \ln \rho}; \quad t \equiv \frac{\pi j_0 a^2}{c^2 E_0} \tau; \quad r/a \equiv \rho$$

Critical field model and prior work



Damping of relativistic electron beams by synchrotron radiation
 F. Andersson, P. Helander, and L.-G. Eriksson, *Phys. Plasmas* **8**,
 5221 (2001)



Microinstabilities

❑ Can microinstabilities enhance runaway scattering?

“Fan” instability observed experimentally:

V.V. Alikeev et al., *Sov. J. Plasma Phys.* **1**, 303 (1975).

Modes of interest:

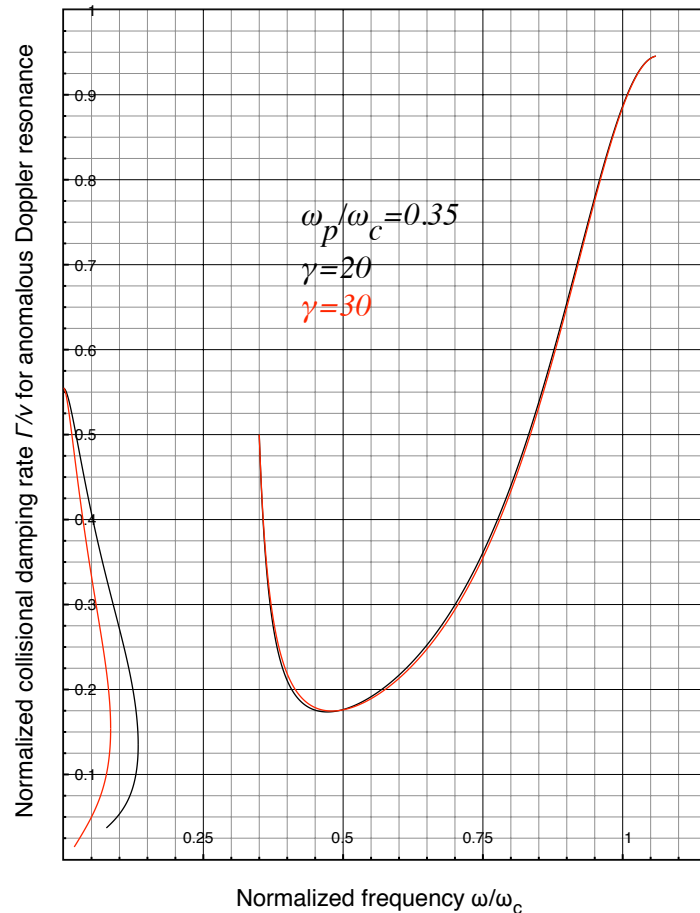
❑ Electron cyclotron (upper hybrid) waves: $\omega = \sqrt{\omega_c^2 + \omega_p^2}$

❑ Magnetized plasma waves: $\omega = \omega_p \frac{|k_{\parallel}|c}{\sqrt{k^2 c^2 + \omega_p^2}}$

❑ Whistlers: $\omega = |\omega_c| \frac{|k_{\parallel}|kc^2}{\omega_p^2 \sqrt{1 + k^2 c^2 \omega_c^2 / \omega_p^4}}$

❑ Waves can be excited via anomalous Doppler resonance ($\omega + |\omega_c| / \gamma = k_{\parallel} V_{\parallel}$) and Cherenkov resonance ($\omega = k_{\parallel} V_{\parallel}$).

Collisional damping for resonant modes



- ❑ Collisional damping and instability threshold have been overestimated in prior work by other authors
- ❑ Collisional damping exhibits significant frequency dependence
- ❑ Whistler mode has the lowest damping rate

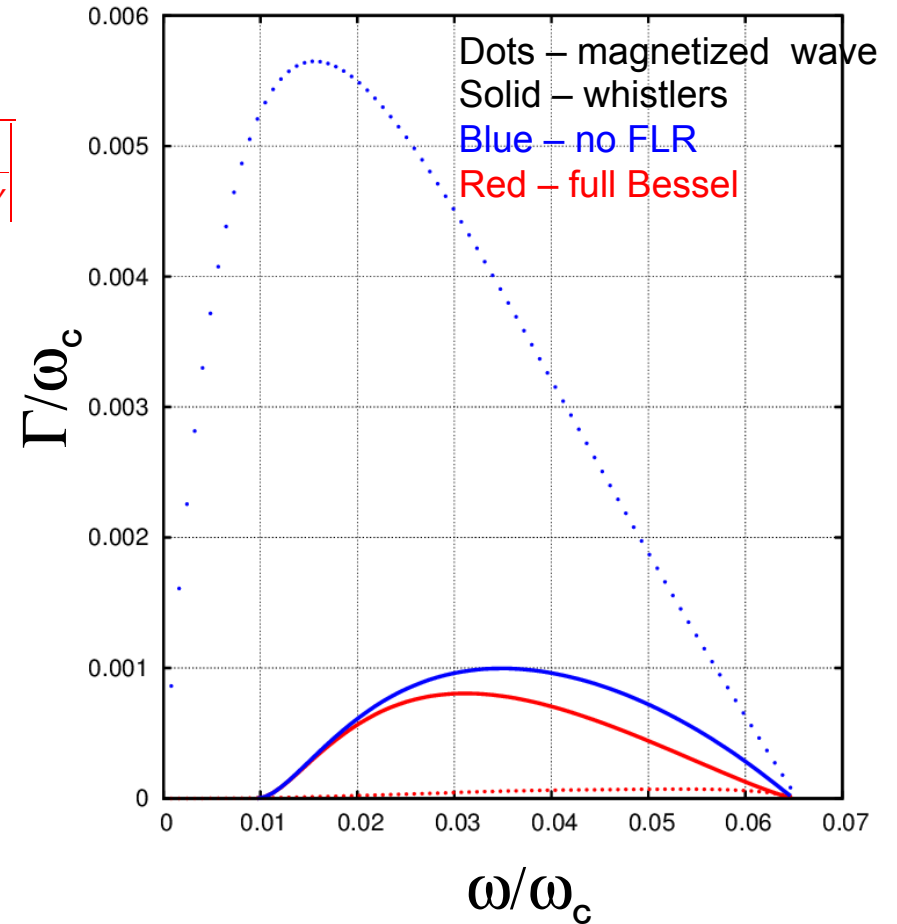
Damping rates for waves driven via anomalous Doppler resonance

Kinetic drive

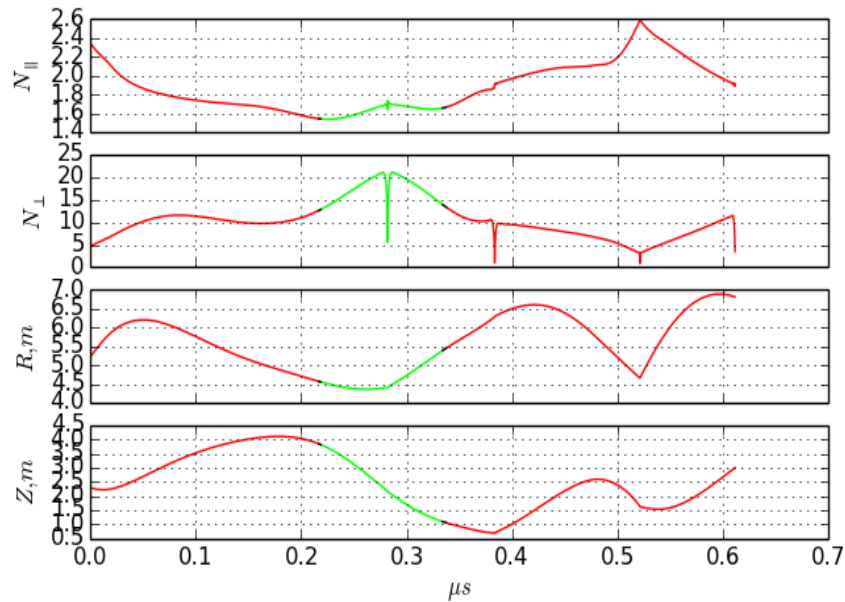
$$\frac{\Gamma}{|\omega_c|} = R(\omega; \gamma) \frac{2\pi m c \gamma \int p^2 F_b \theta d\theta}{n} \approx R(\omega; \gamma) \frac{n_b}{n}$$

$$R \equiv \frac{\frac{\pi}{4} \frac{\omega_p^2}{\gamma |\omega_c|} \left\{ 1 + i e_2 + e_3 \frac{k_{\perp} c}{\omega_c} \sqrt{\gamma^2 - 1} \right\}^2}{(1 - e_2^2) \left[\omega + \omega \frac{\omega_p^2 \omega_c^2}{(\omega^2 - \omega_c^2)^2} \right] - i e_2 \frac{|\omega_c| \omega_p^2 (\omega^2 + \omega_c^2)}{(\omega^2 - \omega_c^2)^2} + \omega e_3^2 \sqrt{\frac{\gamma^2 - 1}{\gamma^2} - \frac{k_{\parallel} c}{\omega_c \gamma}} \frac{1}{|\omega_c|}}$$

- ❑ The drive for whistlers from a narrow electron beam is weaker than the drive for the magnetized plasma branch
- ❑ Finite Larmor radius effect suppresses magnetized plasma waves
- ❑ Whistlers have the lowest collisional damping



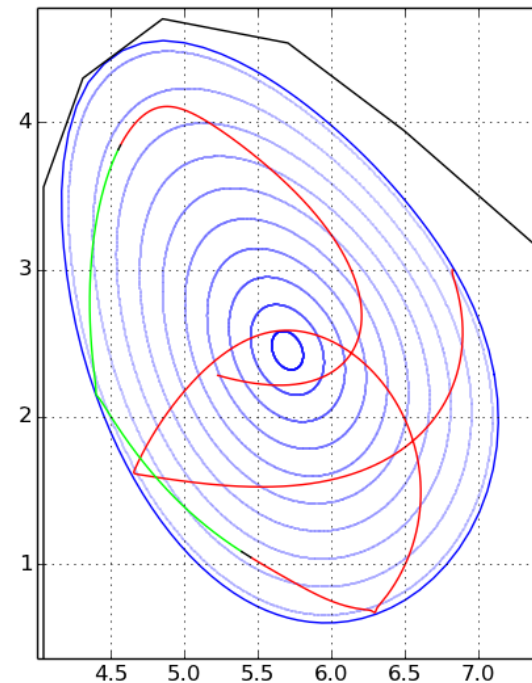
Ray tracing shows internal reflection and linear transformations of wave packets



Wave packet transformation

Red curve - whistler wave

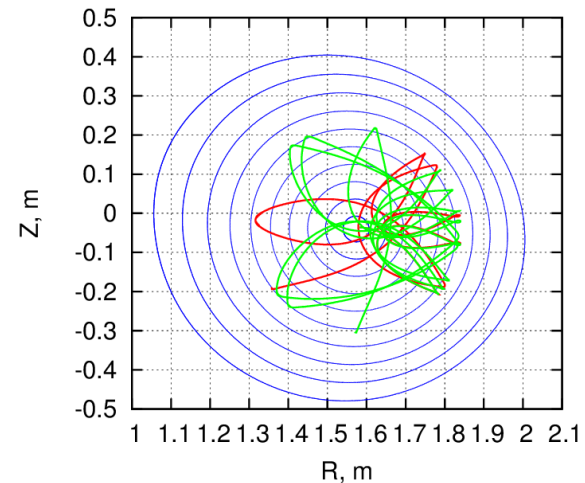
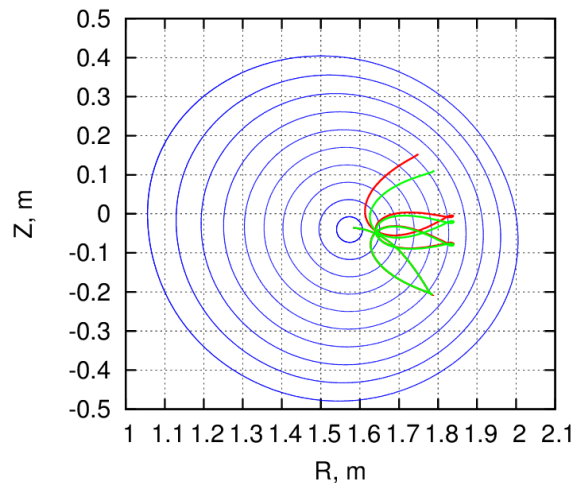
Green curve - magnetized
plasma wave



Poloidal motion
of the wave packet

Statistical analysis

Wave trajectories diverge after multiple reflections and due to small fluctuations of plasma parameters



This randomness calls for statistical analysis:

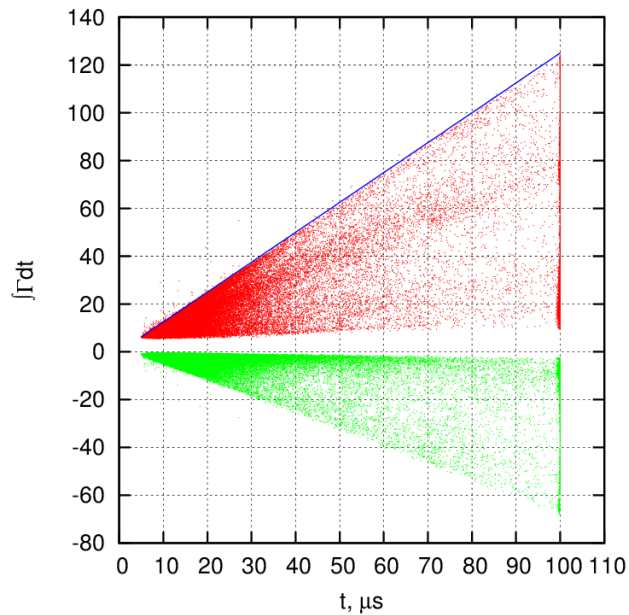
1. Launch many waves at a reference temperature
2. Calculate drive and damping separately and find trajectories with maximum amplification factor
3. Scale damping with temperature
4. Find minimal temperature for instability to appear.

Simulation results for ITER parameters

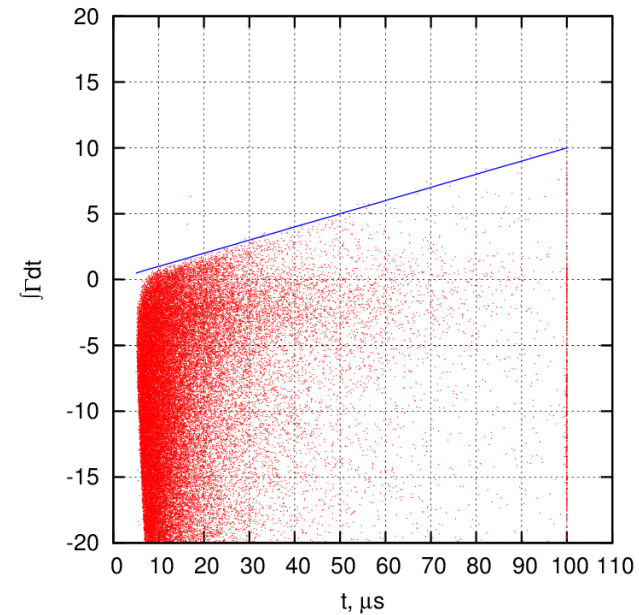
$$n_e \sim 1.3 \cdot 10^{20} \text{ m}^{-3} \quad T_e \sim 22 \text{ eV} \quad j_{re} \sim 1.0 \text{ MA} / \text{ m}^2 \quad E_{re} \sim 15 \text{ MeV}$$

Fast analysis of several million wave packets
determines instability onset

Kinetic drive and damping



Total amplification factor



The local growth rate at the plasma core becomes positive at $T_e \sim 12 \text{ eV}$
Ray-tracing analysis requires higher temperature for the instability onset.

Nucl. Fusion **55**, 043014 (2015).

Summary

- ❑ Self-consistent kinetic modeling of primary runaway formation during thermal quench (prompt conversion of the plasma current into runaway current is advantageous for plasma position control).
- ❑ Kinetic near-threshold theory for runaway sustainment and runaway avalanche in presence of synchrotron losses (enhanced critical electric field found for avalanche onset).
- ❑ Marginal stability scenario for runaway-dominated current quench (runaway avalanche threshold determines the current decay time-scale).
- ❑ Revised thresholds of runaway-driven micro-instabilities (instability window quantified for ITER-relevant parameters).